Research Paper

Predictions of Onset of Crystallization from Experimental Relaxation Times I-Correlation of Molecular Mobility from Temperatures Above the Glass Transition to Temperatures Below the Glass Transition

Chandan Bhugra,[1] **Rama Shmeis,**[2,3] **Steven L. Krill,**[3] **and Michael J. Pikal**[1,4]

Purpose. Predicting onsets of crystallization at temperatures below T_g, from data above T_g, would require that the correlation between crystallization onset and mobility is same above and below T_g, and the techniques being used to measure mobility above and below T_g are measuring essentially the same kind of mobility. The aim of this work is to determine if the relaxation times obtained using different techniques (DSC, TAM) below T_g correlate with relaxation time obtained above T_g using dielectric spectroscopy.

Methods. Model compounds for this work were chosen based on their varied ΔH_f, $\Delta C_p(T_g)$ and H-bonding in crystalline state *vs.* amorphous state. Relaxation times above T_g were determined by the simultaneous fit of real and imaginary permittivity to the Cole-Davidson model. Tau and beta below T_g were determined using isothermal microcalorimetry (TAM) or MDSC. MDSC was used to calculate Kauzmann temperature and strength of the glass using established relationships.

Results. Indomethacin, nifedipine and flopropione showed Arrhenius temperature dependence throughout the entire temperature range and extrapolation of τ^β measured above T_g by dielectric relaxation agreed with τ^β measured below T_g by TAM/MDSC. Ketoconazole, however, showed the expected VTF behavior. For at least two compounds compared (indomethacin and ketoconazole), relaxation times measured by TAM and MDSC did not agree, with TAM giving significantly lower values of τ^β, but TAM and MDSC relaxation times appeared to extrapolate to a common value at T_g.

Conclusions. It was found that, for all cases studied, relaxation time constants determined above and below T_g did appear to extrapolate to the same value around T_g indicating that molecular mobility measured above and below T_g using different techniques is highly correlated.

KEY WORDS: amorphous pharmaceuticals; calorimetry (DSC); calorimetry (TAM); Cole Davidson model; crystallization; dielectric relaxation; glass transition; heat capacity; molecular mobility; physical stability; relaxation time.

INTRODUCTION

Formulation of new drug candidates is becoming increasingly difficult due to the low solubility associated with them. In such cases, the amorphous state is extremely appealing. Being a high-energy state, it offers the advantage of higher solubility and perhaps enhanced bioavailability through improved dissolution (1). However, this high energy comes with its own price of higher instability, both chemical and physical (2,3), which may preclude the use of amorphous state in solid oral dosage forms. Instability in amorphous matrices, particularly physical instability or crystallization from amorphous state, has often been linked to the molecular mobility of these systems (4). This link between the mobility of the amorphous matrix and instability can perhaps be exploited to make sensible predictions at temperatures of pharmaceutical relevance where reaction rates are greatly reduced. Such calculations would involve establishment of coupling between reaction rates, i.e., crystallization onset or growth rates, and relaxation time of the amorphous matrix at higher temperatures and extrapolating such correlations to lower temperatures. If such a relationship exists, the information would help develop an accelerated stability testing protocol to assess crystallization from the amorphous matrix. However, to validate this approach, we first need to measure the molecular mobility of the amorphous matrix over a broad temperature range from temperatures above the glass transition to temperatures below the glass transition. Use of a single technique (considering instruments available in most laboratories) does not provide the required information for the entire temperature range. Previous work, i.e., Carpentier *et al.*, showed correlation of relaxation times

[1] Department of Pharmaceutical Sciences, School of Pharmacy, U-3092, University of Connecticut, 69 North Eagleville Road, Storrs, Connecticut 06269, USA.
[2] *Present address*: Pharmaceutical Sciences Department, Sanofi-Aventis, 1041, Route 202-206, P.O. Box 6800, Bridgewater, New Jersey 08807-0800, USA
[3] Pharmaceutical R&D, Boehringer Ingelheim Pharmaceuticals, Inc., 900 Ridgebury Rd., P.O. Box 368, Ridgefield, Connecticut 06877, USA.
[4] To whom correspondence should be addressed. (e-mail: pikal@uconnvm.uconn.edu)

obtained using two techniques, specific heat spectroscopy (MDSC—determining the real and imaginary components of specific heat over one decade of frequency) and dielectric spectroscopy (5), correlating the relaxation times at temperatures above the glass transition. However, these measurements were not made over a sufficient temperature range to address the extrapolation procedure in which we have interest (i.e., to well below T_g). In order to develop the stability testing protocol for the instability of interest, i.e., crystallization from the amorphous state, we extend the correlations to below the glass transition temperature using calorimetry for measuring relaxation times below the glass transition temperature and dielectric relaxation spectroscopy for measuring relaxation times above the glass transition temperature. (Previous unpublished work from our lab suggested that such correlations exist for a hydrophilic compound (sucrose) but the same was limited to a single observation (6)).

The model compounds chosen for this study represent factors that may impact crystallization from the amorphous state. Such factors include the heat of fusion, heat capacity change at the glass transition temperature and hydrogen bonding towards or away from the structure in crystalline lattice. Table I gives the compounds chosen with the respective parameter italicized. Indomethacin (MW 357.8) was chosen due to the wealth of information on this compound. Ketoconazole (MW 531.4) had the highest heat of fusion on a molar basis. Heat of fusion is a measure of the strength of bonds in the crystal lattice, and therefore might be relevant to nucleation and crystal growth rates. Heat capacity change at the glass transition is often correlated with the strength of glass former with higher heat capacity change correlated with higher fragility (where fragile liquids show non-arrhenius temperature dependence of relaxation times above T_g) (7). However, there are some exceptions such as certain hydrogen bonded liquids (8) and a case recently presented by Angell *et al.* in which they showed lower $\Delta C_p(T_g)$ for decalin with high fragility (9). Flopropione (MW 182.2) was chosen because of the high $\Delta C_p(T_g)$ associated with this compound. Hydrogen bonding differences between amorphous and crystalline states could also be an important factor in crystallization from the amorphous state. Stronger hydrogen bonding in the amorphous state may delay crystallization and vice versa. Tang *et al.* evaluated the strength of hydrogen bonding in various dihydropyridines using FTIR and Raman spectroscopy in combination with X-ray crystal structure data (10). We study two of the compounds, one where hydrogen bonding is stronger in the crystalline state (nifedipine, MW 346.3) and the other where hydrogen bonding is stronger in the amorphous state (felodipine MW 384.6).

MATERIALS

Indomethacin was purchased from Sigma Aldrich. Nifedipine and ketoconazole (USP grade) were purchased from Professional Compounding Center of America. Flopropione was purchased from TCI America. All compounds were used without further purification. Amorphous samples were prepared by heating the crystalline substance 10°C above the melting point and quenching the melt with liquid nitrogen. Unpublished results from our lab suggests that small amounts of mechanical stress in the amorphous state below the glass transition temperature can result in introduction of nuclei and can affect crystallization behavior both above and below T_g (11). Considering the importance of mechanical stress in determining the crystallization behavior from the amorphous state, all samples were prepared in the sample holder required for measurement and no mechanical stress, except that due to liquid nitrogen quenching was employed. Purity after melt quench was verified using stability indicating HPLC assays (12–15). Percent recovery after melt quench was determined on the basis of a standard curve. For Indomethacin, ketoconazole, nifedipine and flopropione recovery was determined to be 100.3 ± 0.6, 100.7 ± 1.0, 99.69 ± 2.1 and 98.54 ± 0.6%, respectively. No new peaks were found in indomethacin, ketoconazole and nifedipine; however, flopropione showed slight degradation and a peak with retention time higher than that of the parent drug.

METHODS

### Dielectric Relaxation Spectroscopy

Dielectric Relaxation Spectroscopy (DRS) has been shown to be a very useful technique to probe molecular motions particularly because of its ability to cover a wide frequency range (μHz–GHz) (16,17). Depending on the available frequency range, one can study relaxations in both the glassy state (at least, in principle), where the mobility is slow, as well as in the supercooled liquid state where mobility is faster (18–20). Recently dielectric relaxation spectroscopy has been used to study isothermal crystallization of amorphous substances (21). However, for this research DRS was used to explore the molecular mobility at and above the glass transition temperature. For the purpose of measuring relaxation time as a function of temperature a time domain spectrometer (TDS, IMASS, MA, USA) was used (22). This instrument measures the response of the material to an externally applied field as a function of time. The equivalent

Table I. Glass Transition Temperature (T_g), Heat Capacity Change at Glass Transition [$\Delta C_p(T_g)$], Heat of Fusion (ΔH_f) and Hydrogen Bonding Characteristics (Nifedipine and Felodipine, Data from Literature) for the Model Compounds

S. No.	Name	T_g (°C)	ΔC_p (J/g/°C)	ΔH_f (J/gm)	H-bonding Stronger
1	Indomethacin	44.2 ± 0.2	0.46 ± 0.02	108 ± 3	–
2	Ketoconazole	42.9 ± 0.1	0.46 ± 0.02	*96 ± 3*	–
3	Nifedipine	41.4 ± 0.04	0.42 ± 0.01	119 ± 4	*In crystal*[a]
4	Flopropione	58.3 ± 0.1	*0.75 ± 0.02*	165 ± 1	–
5	Felodipine*				*In amorphous*[a]

Each compound is associated with a parameter italicized indicating the rationale for studying that compound.
[a] Indicates data from literature [10].
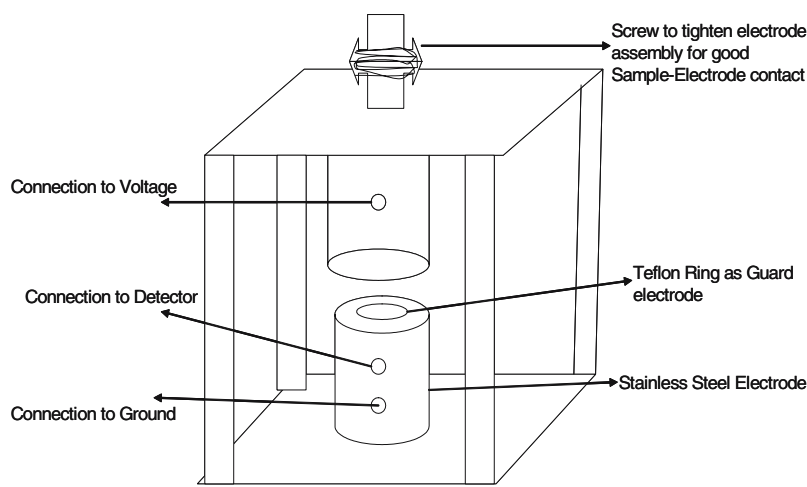
Electrode Assembly

Fig. 1. Electrode assembly for dielectric measurement.

frequency range is 10^{-4} to 10^4 Hz. A step voltage is applied to the sample and the response is measured as a function of time and is subsequently converted into the frequency domain using Laplace transformation. An equal and opposite voltage is applied to the reference capacitor to subtract the initial rapid response to the applied field. The transient difference in the capacitance of the sample and reference is measured by a charge amplifier.

The electrode assembly required for these experiments was developed by the staff of the Institute of Material Science (Machine Shop IMS, University of Connecticut). The schematic of the electrode assembly is given in Fig. 1. The construction consists of a parallel plate electrode made of stainless steel. For the purpose of these experiments the samples, 0.8–1.0 g, were prepared by melting the crystalline sample in an aluminum weighing pan by heating 10°C above the melting point and then quenching the sample to a thin disc with a steel bar dipped in liquid nitrogen (the weight of the steel bar ensures a plane surface of uniform thickness). This method resulted in samples of approximately 0.3- to 0.5-mm thickness. All sample preparations were performed in a dry nitrogen atmosphere. The electrode was guarded with a built-in Teflon ring to prevent the effects of stray

capacitance, edge effects, and conductance due to adsorption of water by hygroscopic materials. The screw at the top of the assembly ensured that there is good contact between the sample and electrode, and it also removes air gaps. Electrodes of two different sizes were used depending on the response of the sample to the applied field. The overall response, given by capacitance (C), depends on the sample characteristics (permittivity ε) and the geometry of the sample. The relation between capacitance and sample geometry is given in Eq. (1) and shows that capacitance is directly proportional to the size of the electrode (area, A) and inversely proportional to the thickness (d) of the sample.

$$C = \frac{A\varepsilon}{d} \qquad (1)$$

For indomethacin and ketoconazole, a larger electrode was used (diameter 2.4 cm), and for nifedipine and flopropione a smaller electrode was used (diameter 1 cm). The whole electrode assembly was placed in an external temperature controller (Delta Design 9023, range −150 to 250°C, temperature control ± 0.2°C). The sample was subjected to a step voltage (10 V) which resulted in polarization of the dipoles present in the sample. Before application of the voltage, a
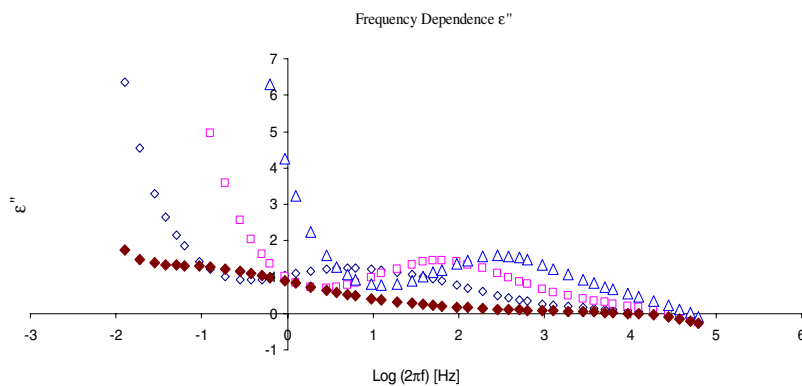
Frequency Dependence ε″

Fig. 2. Frequency dependence of imaginary permittivity (ε'') as a function of temperature for Ketoconazole. *Filled diamonds*, *open diamonds*, *squares* and *triangles* represent 45, 50, 55 and 60°C, respectively.

baseline measurement was performed, and the baseline was subtracted from the final response, as the baseline was indicative of the drifts in detector currents.

By performing the experiment at four to five different temperatures (at and above the T_g every 5°C), mobility parameters were evaluated as a function of temperature. A representative curve for the frequency dependence of the imaginary component of permittivity for ketoconazole is given in Fig. 2. The figure clearly shows that, with increase in temperature, the peak of the imaginary component of permittivity shifts to higher frequency, indicating a decrease in relaxation time with increase in temperature.

Dielectric Relaxation Data analysis

Debye in 1929 first described the frequency response of dielectrics (23). The empirical model, developed by Debye was further improved by Cole–Cole (24), Cole–Davidson (25) and Havriliak–Negami (26) to account for different shapes seen in different compounds. Cole–Cole also showed that for a material exhibiting Debye relaxation a plot of imaginary permittivity (ε'') against real permittivity (ε'), with each point corresponding to a particular frequency, would yield a semicircle (24). However, such plots almost always show contributions from dc conductivity, such effects being more prominent at low frequencies (27). A representative Cole–Cole plot for supercooled Indomethacin at 65°C is shown in Fig. 3, where the spike in imaginary component seen at low frequencies suggests contribution from dc conductivity, which compromises use of the instrument at temperatures below T_g. Since the dc effect is not due to dipolar relaxation, it is not considered and is removed prior to further analysis. Another important observation depicted from such plots is the shape (asymmetric) of the plots, first observed for glycerol by Cole and Davidson (25,28). The asymmetric shape of the curve obtained in Fig. 3 shows the similarity of the dielectric behavior of the compounds we study with the behavior reported by Cole and Davidson, and therefore the Cole–Davidson equation was used for obtaining the relaxation parameters (i.e., since the

equations are empirical, modification to the original Debye equation were made to account for different shapes observed).

The remaining set of data was analyzed using the Cole–Davidson Model for dielectric relaxation as given in Eq. (2), including a term for dc conductance (i.e., in this way we accounted for the contribution of dc conductivity to the dipolar relaxation for the entire frequency range):

$$\varepsilon^* = \varepsilon_\infty + \frac{\varepsilon_S - \varepsilon_\infty}{(1 + i\omega\tau)^\beta} + \frac{\sigma_{dc}}{i\omega\varepsilon_S} \qquad (2)$$

In the above equation ε^* is the complex permittivity, ε_S is the low frequency limit of permittivity, ε_∞ is the high frequency limit, ω is the frequency ($2\pi f$), τ the relaxation time, β represents the distribution of relaxation times with a value close to unity indicating homogenously distributing species and values close to zero indicating broad distribution of relaxing sub-states, σ_{dc} is the dc conductivity contribution. The relaxation parameters, τ and β, were obtained by simultaneous fitting of the real and imaginary components of the Cole–Davidson equation to the data using a nonlinear fitting program (Origin 5.0). For the purpose of simultaneous fitting, Eq. (2) was rewritten to give equations for real and imaginary components of permittivity [given in Eqs. (3) and (4)] (25),

$$\varepsilon' = \varepsilon_\infty + (\varepsilon_S - \varepsilon_\infty)\left[\cos\left\{\tan^{-1}(\omega\tau)\right\}\right]^\beta\left[\cos\left\{\beta^*\tan^{-1}(\omega\tau)\right\}\right] \qquad (3)$$

$$\varepsilon'' = (\varepsilon_S - \varepsilon_\infty)\left[\cos\left\{\tan^{-1}(\omega\tau)\right\}\right]^\beta\left[\sin\left\{\beta^*\tan^{-1}(\omega\tau)\right\}\right] - \frac{\sigma_{dc}}{\varepsilon_S\omega} \qquad (4)$$

In the above equations all the symbols have their usual meaning and were defined earlier. Figure 4 gives one such plot showing the simultaneous fitting of the Cole–Davidson equation to the data. Note that the fit is essentially perfect. Table II gives the values of τ^β and beta values (for above T_g range) measured for all the compounds, both above the glass transition and below the glass transition, where dielectric
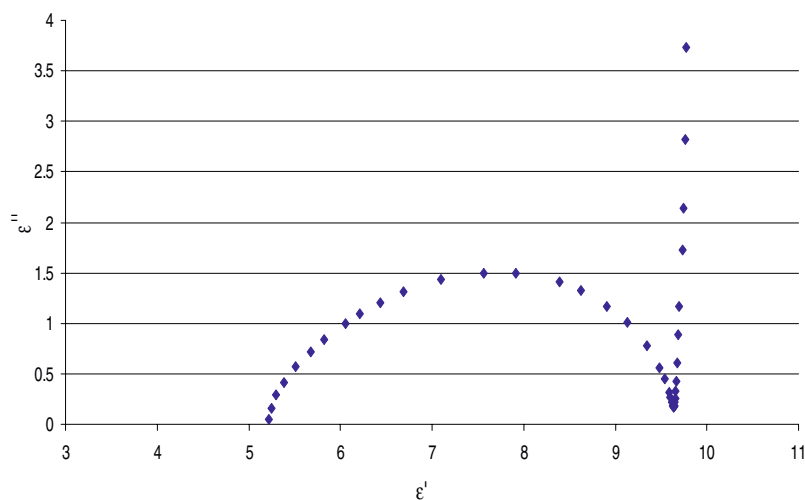
Fig. 3. Cole–Cole plot for indomethacin at 65°C. Spike at low frequency (large ε', real permittivity) is contribution from dc conductivity.
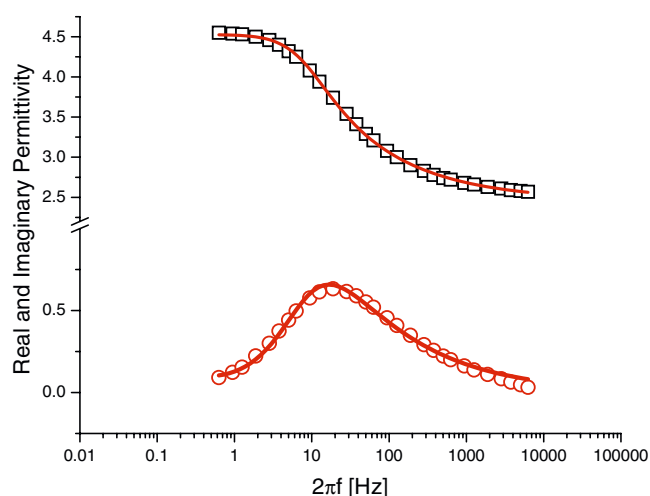
Fig. 4. Simultaneous fitting of the real and imaginary components of the Cole–Davidson model to the real (*squares*) and imaginary (*circles*) permittivity of indomethacin at 55°C. $\chi^2 = 0.00037$, $\varepsilon_S = 4.52 \pm 0.007$, $\varepsilon_\infty = 2.45 \pm 0.012$, $\tau = 0.12 \pm 0.003$ s and $\beta = 0.41 \pm 0.008$. *Lines* connecting the points are the fitted lines obtained from nonlinear curve fitting using origin software.

relaxation was employed above T_g and calorimetry was used below T_g.

Differential Scanning Calorimetry

DSC 2920 and DSC Q1000 calorimeters from TA Instruments (New Castle, DE, USA) equipped with refrigerated cooling systems were used. DSC was used both in standard mode and in modulated mode to determine the parameters of interest. The system was calibrated for temperature and cell constant using high purity Indium when used in standard mode (ramp rate 10°C/min) for accurate measurement of the heat of fusion of crystalline samples. For this purpose approximately 10 mg of the sample was pressed in aluminum hermetic pans (pin holes were made in these hermetic pans) from TA Instruments. The heats of fusion of model compounds are given in Table I.

For use in the modulated mode, the system was calibrated for temperature and cell constant using high purity indium and for heat capacity using crystalline sucrose. The modulation parameters used were amplitude ± 1°C, frequency 100 s and ramp rate 1°C/min. For the purpose of these experiments, the following values of heat capacity constants were used $K_{C_{P_{\text{TOTAL}}}} = 1.17$, $K_{C_{P_{\text{REV}}}} = 1.28$. The heat capacity values obtained with these constants for the compounds under study were close to values found in the literature. The following parameters were determined using DSC in modulated mode:

• Determination of T_g and ΔC_p (T_g) and other glassy state parameters: Roughly 5–10 mg of crystalline sample was carefully pressed in hermetic aluminum pans from TA Instruments (pin holes were made in these hermetic pans). The heat capacity of crystalline sample was measured using the modulation parameters described above. Vacuum-dried crystalline samples were used in order to ensure removal of trace levels of solvent. Since the heat capacity difference between crystalline and amorphous sample is only 5–10%, these differences were very sensitive to sample weight and packing. For this reason, measurements on both crystalline and amorphous systems were made on the same sample. The same sample was heated to the melt and then quenched to measure the heat capacity of the amorphous solid and the supercooled liquid. A representative plot showing the difference in reversing heat capacity of crystalline and amorphous solid for Ketoconazole is shown in Fig. 5. The glass transition temperature was determined as the mid point of the step change in reversing heat capacity at T_g (determined using Universal Analysis Software, TA Instruments, version 4.1). The heat capacity change at T_g (ΔC_p) was determined using linear fits to the reversing heat capacity of the supercooled liquid and glass extrapolated to T_g. Values of $\Delta C_p(T_g)$ and T_g for three different measurements with standard deviation are given in Table I.

• Determination of Enthalpy Recovery as a function of time and temperature: Enthalpic recovery was determined as a function of annealing time at various temperatures below the glass transition temperature. Initially we wanted to use

Table II. Dielectric and Calorimetric Relaxation times, τ^β (Tau in Hours) at the Temperatures Studied for the Given Compounds

Temperature (°C)	Indomethacin τ^β (h)	Ketoconazole τ^β (h)	Nifedipine τ^β (h)	Flopropione τ^β (h)
Calorimetric	Isothermal Microcalorimetry		Modulated DSC	
15			70 ± 10	
20		3.3 ± 1.1	20 ± 6	
25	3.4 ± 0.3	3.1 ± 0.6	11 ± 2	
30	1.5 ± 0.6	1.8 ± 0.2		
35	0.34 ± 0.08	0.9 ± 0.2		32 ± 5
40				9.2 ± 1.3
45				4.5 ± 0.3
Dielectric	Relaxation Time Around and Above T_g			
45		0.15 ± 0.016 (0.34)	0.058 ± 0.02 (0.45)	
50	0.052 ± 0.012 (0.42)	0.055 ± 0.015 (0.33)	0.011 ± 0.002 (0.50)	
55	0.014 ± 0.0014 (0.42)	0.020 ± 0.002 (0.35)	0.0038 ± 0.001 (0.50)	0.095 ± 0.008 (0.35)
60	0.0061 ± 0.0005 (0.41)	0.011 ± 0.002 (0.35)	0.0013 ± 0.0003 (0.52)	0.029 ± 0.002 (0.38)
65	0.0027 ± 0.0003 (0.41)			0.012 ± 0.0009 (0.37)
70	0.0018 ± 0.0003 (0.40)			0.0046 ± 0.001 (0.38)

Standard deviation is for three separate measurements. Beta value at each temperature for dielectric measurements is given in parenthesis.

Configurational Cp
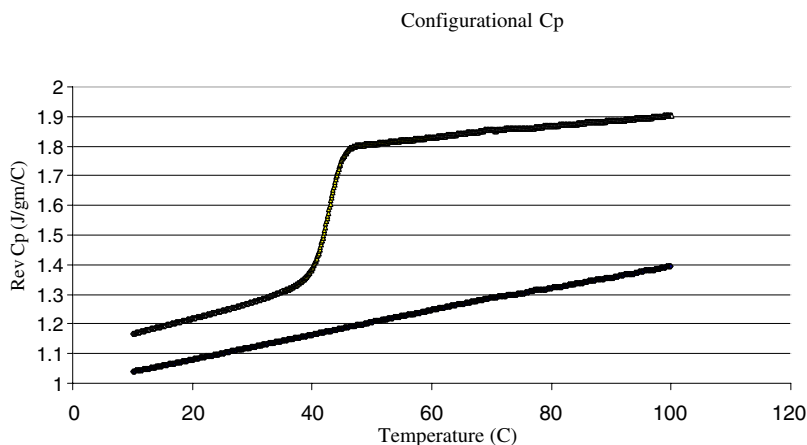
Fig. 5. Reversing heat capacity as a function of temperature for ketoconazole. *Lower line* is the heat capacity of the crystalline ketoconazole and the *upper curve* is for amorphous ketoconazole going through the glass transition.

isothermal microcalorimetry (TAM) for determination of relaxation time below the glass transition temperature. However, it was found that nifedipine started to crystallize in the TAM at temperatures close to the glass transition (30°C and 35°C) before significant relaxation could take place. Thus, the power curve obtained from TAM had contributions due to relaxation and crystallization which could not be separated. For this reason, relaxation parameters for nifedipine were evaluated at lower temperatures using MDSC where the interference from crystallization was minimal. The second compound where MDSC was used to determine the relaxation time was flopropione. Flopropione had traces of solvent left after the manufacturing process (and a very small quantity even after vacuum drying at 25°C for 24 h), and it was difficult to prepare a consistent sample in the TAM ampoule. It is for this reason we used MDSC for evaluating the relaxation parameters for this compound. Later, after it was found that there were differences in the relaxation parameters obtained using different calorimetric techniques (see results and discussion), relaxation times for the other two compounds (indomethacin and ketoconazole) were also determined using MDSC. Comparison between these two calorimetric measures of relaxation times will be discussed in the next section.

For the purpose of determining the enthalpy recovery approximately 7–9 mg of crystalline sample was pressed in aluminum hermetic pans (with pinhole). The samples were heated above the melt temperature and then cooled to below ambient (-40°C) to produce the amorphous samples. Freshly prepared amorphous samples were annealed for various time points in the DSC and the relaxation function was determined using Eq. (5):

$$\phi(t, T) = 1 - \frac{\Delta H(t, T)}{\Delta H(\infty, T)} \qquad (5)$$

where, $\Delta H(t, T)$ was determined by integrating the area under the non-reversing signal obtained for the annealing time point, and correcting for the "frequency effect" as

described later. ΔH(infinity, T) was determined using the following relationship:

$$\Delta H(\infty, T) = \Delta Cp(Tg - T) \qquad (6)$$

In the above equation ΔC_p is the heat capacity change at T_g determined previously, T_g is the glass transition temperature, and T is the temperature of annealing. Nonlinear curve fitting (Origin 5.0) of the empirical KWW equation (29,30) Eq. (7) to the data obtained from Eq. (5) with time gave τ and β:

$$\phi(t, T) = \exp\left[-\left(\frac{t}{\tau}\right)^{\beta}\right], 0 < \beta \leq 1 \qquad (7)$$

In the above equation $\phi(t, T)$ is the relaxation function calculated using Eq. (5), t is the time of measurement in hours, τ is the relaxation time in hours, and β is the stretched exponential parameter reflecting the distribution of relaxation times. Values of beta close to 1 indicate a homogenously relaxing system and small values indicate a wide distribution of relaxing microstates (31). The enthalpic recovery obtained using the described protocol has contributions to annealing due to relaxation during the slow heating ramp rates used in modulated DSC and also due to the frequency used in modulating the heating rate (called as "frequency effect") (32,33). This contribution to annealing was eliminated by subtracting the area of the non-reversing signal obtained at time ($t = 0$) from all other annealing time points (34). Since the frequency effect also depends on the sample size and density (32,33), care was taken to use consistent sample sizes (this ensures equal contribution due to frequency effect in subsequent experiments). A representative plot showing the fitting of the KWW equation to the relaxation function for Flopropione at 40°C is given in Fig. 6.

However, this analysis does not take into account the change in structure of the amorphous system with aging, which is not accounted for in the simple KWW kinetic model. It is known that with annealing the relaxation time, τ, increases (34). The change in relaxation time constant with annealing introduces errors in measurement of both τ and β
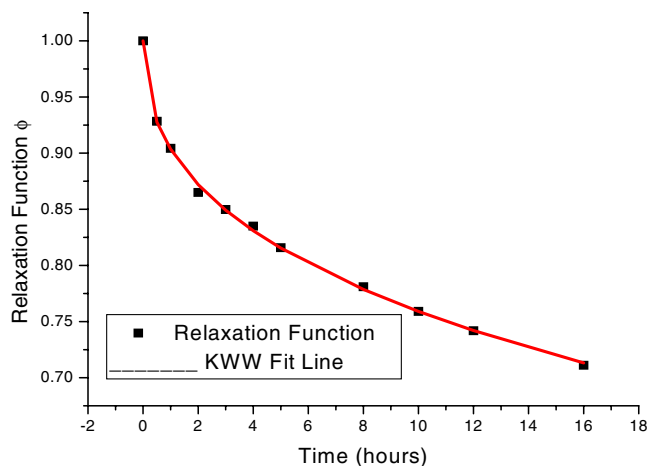
Fig. 6. KWW fitting shown for Flopropione at 40°C. The relaxation parameter was obtained using the protocol described in the text. The connecting *line* is from the fitting of the KWW equation to the relaxation data. $\chi^2 = 2e-05$; $\tau = 190 \pm 21$ h; $\beta = 0.44 \pm 0.01$.

which are in opposite directions such that values of τ are too high and β too low, however the value of τ^β obtained by the analysis *does* represent the value of τ^β for the starting sample and is generally a more robust quantity (34,35). Therefore, for this work we will use τ^β for comparison between different relaxation times. Table II gives the relaxation times for nifedipine and flopropione at various temperatures. Standard deviations are for three independent measurements.

Isothermal Microcalorimetry (Thermal Activity Monitor)

TAM has been used to study the relaxation behavior of amorphous pharmaceuticals (35,36). This technique provides a direct measure of the rate of energy gain or loss as a function of time during annealing. Drug samples, 200–250 mg, were prepared in glass ampoules (4 ml thermometric) and sealed in atmosphere of dry nitrogen. The samples were heated above the melting point and quench-cooled in a liquid nitrogen bath. Crystalline glycine was used as the reference in the TAM. The power time curve obtained as a result of relaxation in the sample was evaluated using the derivative form of the "modified stretched exponential" (MSE) equation (35).

$$P = 277.8 \frac{\Delta H_r(\infty)}{\tau_0} \left(1 + \frac{\beta t}{\tau_1}\right) \left(1 + \frac{t}{\tau_1}\right)^{\beta-2}$$
$$\exp\left[-\left(\frac{t}{\tau_0}\right)\left(1 + \frac{t}{\tau_1}\right)^{\beta-1}\right] \quad (8)$$

In the above equation P is the power (in μW/gm), $\Delta H_r(\infty)$ is the enthalpy relaxation at time infinity obtained using Eq. (6), 277.8 is a numerical factor due to conversion of units, τ_0 is the relaxation time constant, τ_1 is the relaxation time constant for the "short time limit", t is measurement time in hours, β represents the distribution of relaxation times. We note that the raw TAM data cannot be used at very small times as the data for $t < 0.5$ h contain contributions from friction produced during insertion of sample and reference ampoules into the measurement position. Also, note that

time zero for the relaxation run is the time when the sample was brought to the temperature of the TAM run, not just when the sample was placed into the measurement zone. Adjustment in time was therefore made to account for the time spent by the sample in the thermal equilibration position (generally 30 min, at temperatures 25, 30 and 35°C). For samples studied at 20°C in the TAM (temperature close to room temperature), time zero was chosen as the time when the sample was prepared, in this case 30 min before introduction into the calorimeter (i.e., a total time adjustment of 1 h). Relaxation parameters (τ_0, τ_1 and β) were obtained from nonlinear curve fitting (Origin 5.0) of Eq. (8) to the power–time data. Relaxation time (τ_D) was obtained from the parameters evaluated from the fit (τ_0 and τ_1) using the following expression:

$$\tau_D = (\tau_0)^{\frac{1}{\beta}}(\tau_1)^{\frac{(\beta-1)}{\beta}} \quad (9)$$

Since relaxation induced errors are also involved in the evaluation of τ_D and β here, we will use τ_D^β as the structural relaxation time parameter. A representative curve showing fitting with the derivative form of the MSE equation Eq. (8) for relaxation in Indomethacin at 30°C is shown in Fig. 7. Obviously, the fit is essentially perfect. Table II gives the values of relaxation times for Indomethacin and Ketoconazole measured with isothermal microcalorimetry for different temperatures. Standard deviation is for three separate measurements unless otherwise noted.

RESULTS AND DISCUSSION

Evaluation of Thermodynamic Parameters of the Glassy State

The heat capacity data generated using modulated DSC was used to evaluate parameters of the glassy state such as configurational entropy, fictive temperature, and the Kauzmann temperature. Table III shows the configurational heat capacity ($= C_p^l - C_p^x$, where C_p^l is the heat capacity of the supercooled liquid and C_p^x is the heat capacity of the crystal)
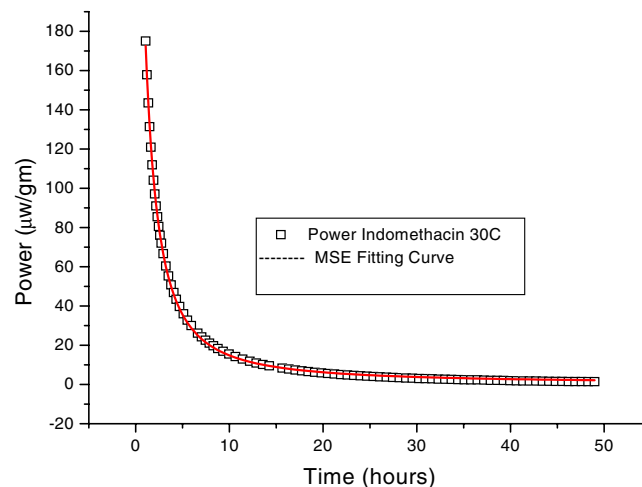
Fig. 7. Power time data from isothermal microcalorimetry for indomethacin at 30°C. The *line* was generated by fitting the derivative of the MSE equation to the TAM data. $\chi^2 = 0.82$; $\tau_0 = 1.45$ h ± 0.009; $\tau_1 = 1.1 \pm 0.006$ h; $\beta = 0.15 \pm 7.9e-04$; $\Delta H_r = 6.55$ J/g.

of all the compounds under study. The configurational heat capacity is significantly higher than the heat capacity change at T_g ($C_p^l - C_p^a$, where C_p^a is the apparent heat capacity of the glass), as shown in Tables I and II, and therefore one cannot assume that the configurational heat capacity is exactly given by the change in heat capacity at T_g (8). The configurational heat capacity of the glass was used to calculate the Kauzmann temperature. Kauzmann was the first to note the existence of a temperature, T_K, above absolute zero where the configurational entropy of the "equilibrium super-cooled liquid" would vanish and where molecular rearrangement will become improbable even at long time scales (37). Taking the configurational heat capacity at T_K as zero and using the temperature dependence of configurational heat capacity one can determine the Kauzmann temperature by the following relationship (8).

$$\frac{1}{T_K} = \frac{1}{T_M}\left(1 + \frac{\Delta H_M}{K}\right) \tag{10}$$

where, ΔH_M is the heat of fusion and K is the constant of proportionality arising from the assumed inverse proportionality between configurational heat capacity and temperature, and is equal to $\Delta C_p(config.)*T_g$. It is important to note that the Kauzmann temperature calculated (T_K) refers to the temperature where the entropy of the super-cooled "equilibrium" liquid becomes equal to the entropy of the crystal (i.e., the extrapolation of the entropy curve from *above*T_g to lower temperatures). However, at T_k, the entropy of the "real" glassy solid is much above that of the crystal, and therefore possesses significant configurational mobility even at T_k. The mobility discussed above is the "global" or "alpha" configurational mobility, which is mobility directly linked to the mobility that drives the glass transition. Local or "beta motion" mobility also occurs below T_g and often at or below T_K. Such effects have been demonstrated by the use of thermally stimulated depolarization current spectroscopy (TSDC), where molecular mobility has been determined at temperatures as low as −160°C for Indomethacin (38). Recently, Vyazovkin *et al.* observed endothermic peaks, attributed to "beta relaxations" in previously annealed samples at temperatures 50°C lower than the glass transition temperature of Indomethacin (39).

The nonzero configurational heat capacity of the glass can contribute significantly to the excess configurational entropy of the glass relative to the liquid as described by Shamblin *et al* (8). Therefore the excess configurational entropy of the non equilibrium glass was calculated as a function of temperature and fictive temperature using the configuration-

al heat capacity data obtained earlier (i.e., $C_p(config) = C_p^l - C_p^x$ in Table III).

$$S_C(T) = \int_{T_K}^{T_f} \frac{C_p(config)}{T}\, dT \tag{11}$$

In this equation $S_C(T)$ is the configurational entropy, T_K is the Kauzmann temperature and T_f is the fictive temperature. The fictive temperature of the glass can be estimated from heat capacity data (8):

$$\frac{1}{T_f} = \frac{\gamma_{Cp}}{T_g} + \frac{1 - \gamma_{Cp}}{T} \tag{12}$$

Where,

$$\gamma_{Cp} = \frac{C_p^l - C_p^g}{C_p^l - C_p^X} \tag{13}$$

A close look at the values of various thermodynamic parameters (Table III) obtained suggests that any analysis made on the basis of just one parameter may not be successful in predicting the overall stability of the amorphous state. For example, Flopropione has the highest configurational heat capacity suggesting the largest difference in configurations between the liquid and the crystal. Thus, one might conclude that flopropione has the highest non-vibrational mobility when compared with the other glass formers studied. This observation also suggests that the system is fragile as per the previous definitions where fragility was associated with change in heat capacity at the glass transition, with higher change in heat capacity indicating higher fragility. However, looking at another parameter, the γC_p function, described previously to be an indicator of strength of the glass former, gives a contradictory view. Shamblin *et al.* suggested a value of γC_p close to unity indicates a strong glass and a small value indicates a fragile glass (8). Flopropione has a value of $\gamma C_p = 0.88$, which is relatively high, and from this criterion, should indicate a strong glass. However, as noted, ΔC_p at T_g is the highest of the materials studied, suggesting a fragile glass. It appears that these two "indicators" of fragility are not equivalent. Note also that the configurational entropy results suggest that flopropione also has the maximum entropic barrier to crystallization (note: configurational entropy is calculated on a per gram basis).

Evaluation of Kinetic VTF Parameters

Evaluation of the kinetic parameters was made using the relaxation time data obtained using dielectric data for

Table III. Thermodynamic Parameters of the Glassy State: Configurational Heat Capacity $\left[C_p^l - C_p^x(T = T_g)\right]$, Thermodynamic Kauzmann Temperature (T_K), Strength Parameter (γ_{Cp}), Strength Parameter (D, VTF Fitting), Configurational Entropy (ΔS_c, Obtained Using Eq. 10) Calculated at T_g and Kinetic VTF Zero Mobility Temperature (T_0, Calculated Using the VTF Fit or Simultaneous VTF as Explained in Text) for Indomethacin, Ketoconazole, Nifedipine and Flopropione

Compound	ΔC_p (Conf) (J/g/°C)	Kauzmann Temperature (°K)	γC_p	D parameter (VTF)	T_0 VTF (°K)	ΔS_c (Conf) (J/g/K)
Ketoconazole	0.62 ± 0.02	282 ± 3	0.75	6.5	269	0.072 ± 0.006
Nifedipine	0.56 ± 0.02	266 ± 4	0.75	6.9	265	0.101 ± 0.008
Indomethacin	0.56 ± 0.06	268 ± 11	0.84	6.9	267	0.100 ± 0.016
Flopropione	0.86 ± 0.09	285 ± 10	0.88	5.9	279	0.135 ± 0.024

temperatures above the glass transition and calorimetric data for temperatures below the glass transition. Since we wanted to include data from both the temperature ranges, i.e., above T_g to temperature range below T_g, to calculate the kinetic zero mobility temperature, we carried out simultaneous curve fitting using the VTF equation for the data above the glass transition range Eq. (14) and the modified VTF equation Eq. (15) for the data below the glass transition temperature.

$$\log \tau^{\beta}(T) = \log \left\{ \tau_0^{\beta} \exp \left(\frac{\beta \cdot DT_0}{T - T_0} \right) \right\} \quad (14)$$

$$\log \tau^{\beta}(T, Tf) = \log \left\{ \tau_0^{\beta} \exp \left(\frac{\beta \cdot DT_0}{T - \left(\frac{T_0}{Tf} \right) T} \right) \right\} \quad (15)$$

In these two equations $\tau(T)$ or $\tau(T, T_f)$ is the temperature-dependent relaxation time, τ_0 is the pre-exponential representing time scale of molecular vibrations (fixed parameter = 2.78E−18 h), β is the distribution of relaxation times and was taken as the average value of the beta from dielectric relaxation (we assume here that β is not dependent on temperature and is therefore constant), D is the Angell's strength parameter (fitting parameter), T_0 is the zero mobility temperature (fitting parameter), T is the temperature and T_f is the fictive temperature calculated using Eqs. 12 and 13. Figure 8 shows the relaxation time data for Ketoconazole obtained by plotting calorimetric (TAM) and dielectric data against reciprocal temperature. VTF parameters are obtained by the simultaneous fit (parameters obtained were $\chi^2 = 0.016$; $B = 1{,}744 \pm 107$; $T_0 = 269 \pm 2.7$ K, figure showing the fit not included). We checked the agreement between the T_0 obtained above with T_0 obtained using only data above T_g and found close agreement between the two values (VTF fitting ketoconazole $T_0 = 263$ K, simultaneous VTF fitting $T_0 = 269$ K). However, we were

successful in using simultaneous fitting for only one compound, i.e., ketoconazole. The reason for not using the data from both the temperature ranges will be discussed later in the correlations section of this paper. For calculating the zero mobility temperature for indomethacin, nifedipine and flopropione only dielectric data from above the glass transition range was used (for this we carried out fitting with VTF Eq. (14) on the relaxation data). Table III shows the comparison between the thermodynamic Kauzmann temperature and the kinetic VTF T_0 temperature. As noted for other systems (40), the agreement is satisfactory suggesting equivalence of thermodynamic and kinetic zero mobility temperatures.

Correlations Between Relaxation Times

Relaxation times obtained using the two techniques was plotted against reciprocal temperature to illustrate correlations between the mobility parameters obtained using different techniques. Figures 8 and 9 give the correlations plotted for all four compounds. Note that, in each case, the dielectric mobility measured at temperatures above the glass transition can be extrapolated to the calorimetric mobility measured at temperatures below the glass transition, suggesting that both measures of mobility are measuring essentially the same type of motion. Figure 8 shows the correlations obtained for ketoconazole, with filled symbols showing relaxation times measured using dielectric spectroscopy and open symbols showing calorimetric τ^{β} measured using the TAM. Ketoconazole shows the expected VTF behavior with a break in slope at the glass transition. The VTF parameters were obtained from the simultaneous fitting of the VTF equation and modified VTF equation, as described previously, to the relaxation data. We note that though we observe a break in slope at the glass transition, the change in slope is not as large as one would expect from theoretical calculations (i.e., using the experimen-

Mobility with Reciprocal Temperature
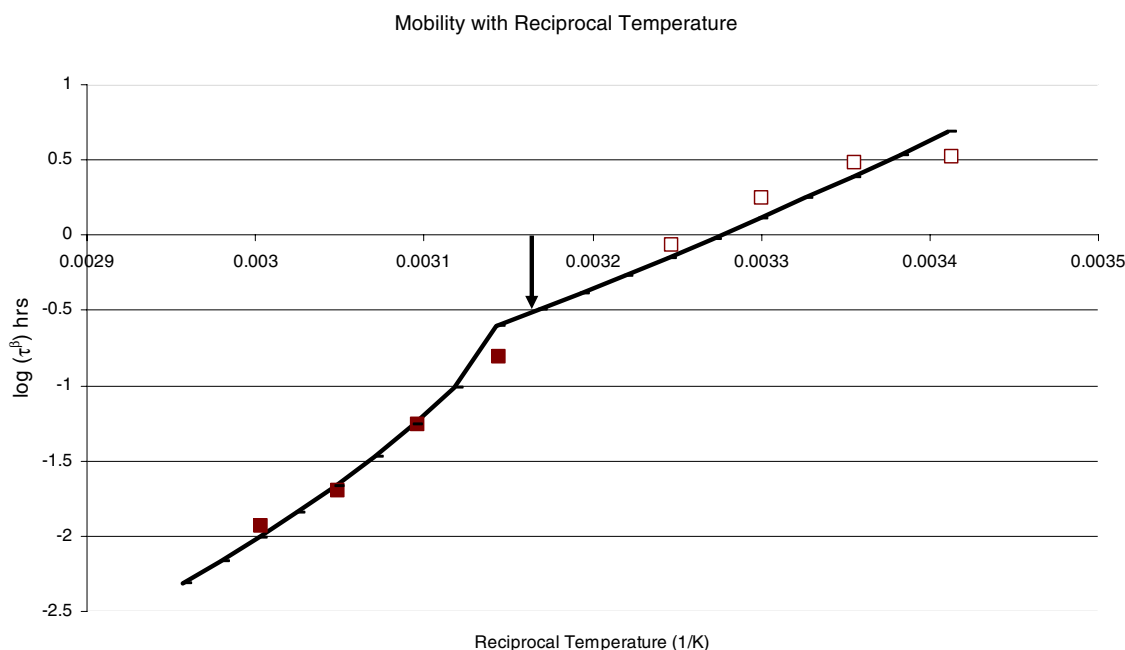
Fig. 8. Correlation of relaxation times for ketoconazole from temperatures above the glass transition to temperatures below the glass transition. *Filled squares* are dielectric relaxation times (τ^{β}), *open squares* are calorimetric relaxation times (τ^{β}, TAM) and the *line* is obtained from the VTF parameters. The *arrow* represents the glass transition.

tal γ_{Cp} value of 0.75). Furthermore, for indomethacin, nifed-ipine (the compound where hydrogen bonding is favored towards the crystalline state), and flopropione (the compound with the largest change in heat capacity at the glass transition) a break in slope at the glass transition is not observable, as illustrated by Fig. 9. Thus, for reasons not understood, the theoretical prediction of the modified VTF equation is not consistent with the data. These compounds, however, do show that the dielectric relaxation time (τ^{β}) and the calorimetric relaxation times are parts of the same curve and in fact, are characterized by the same slope (We do acknowledge that there is some scatter in the data which makes the conclusion of linearity tentative. We also analyzed the dataset using Jacknife's residuals using S-plus statistical software for poten-tial outliers and found no outliers according to Bonferroni Critical Values for 95% confidence intervals). Thus, we do observe a good correlation between dielectric relaxation times measured above T_g and TAM relaxation times measured below T_g. Both techniques appear to predict the same relaxation times near T_g. Such correlations assume that the distribution of relaxation times as given by beta (β) in the KWW Eq. (7), MSE Eq. (8) and Cole Davidson model Eqs. (3) and (4) is the same and there is no significant temperature dependence in beta over the temperature range from above T_g to below the glass transition. In the temperature range above T_g there is no observable temperature dependence in beta (for the temperature range studied as given in Table II). In the temperature range below T_g, use of τ^{β} eliminates the errors in measurement of tau and beta, thus allowing quantitative comparisons of data in the two temperature ranges. Andronis et al. documented similar behavior for Indomethacin where they showed that the dielectric relaxation time (τ) measured in their study (41) could be extrapolated into the calorimetric mobility (τ), measured earlier by Hancock et al. (42) and by Fukuoka et al. (43), *without* a break in slope at the glass transition. In fact, the dielectric and shear relaxation times

measured by Andronis et al. did extrapolate to the calorimetric relaxation times measured previously, following the VTF line. It was only at temperatures much below the glass transition (approximately 25°C below T_g, 293 K), that Andronis et al. observed the change in slope which was significantly less than what was expected from theoretical calculations. However, it is also important to note that annealing induced measurement errors in calorimetric tau and beta were not known at the time the above work was published and hence were not accounted for in the data analysis.

Deviation from the predictions of the modified VTF equation is puzzling, and we have no convincing explanation. Is this deviation a function of technique used? Are different techniques measuring different aspects of mobility or is this the question of sensitivity of the instrument used? Dielectric spectroscopy measures rotation of dipoles, and calorimetry measures, nominally, motion coupled with viscosity and the glass transition, which is mostly translational and whole mole-cule rotation. Thus, while there is a fundamental difference between the types of mobility being measured, it is not obvious that this difference would produce the behavior observed. Rather, we might have expected a significant difference or offset in relaxation time extrapolated to T_g using the two techniques.

Comparison Between Different Measures of Calorimetric Mobility

Isothermal microcalorimetry is more sensitive than scanning calorimetry (MDSC), and there is a possibility that the TAM could be measuring some faster modes of motion in addition to those measured by enthalpy recovery (i.e., those that are mobilized at the glass transition). Thus, we carried out some comparisons between the two measures of calori-metric mobility, TAM and DSC. While previous work demonstrated similarity between the two techniques, that comparison was limited to one hydrophilic compound, i.e.,

Mobility with Reciprocal Temperature
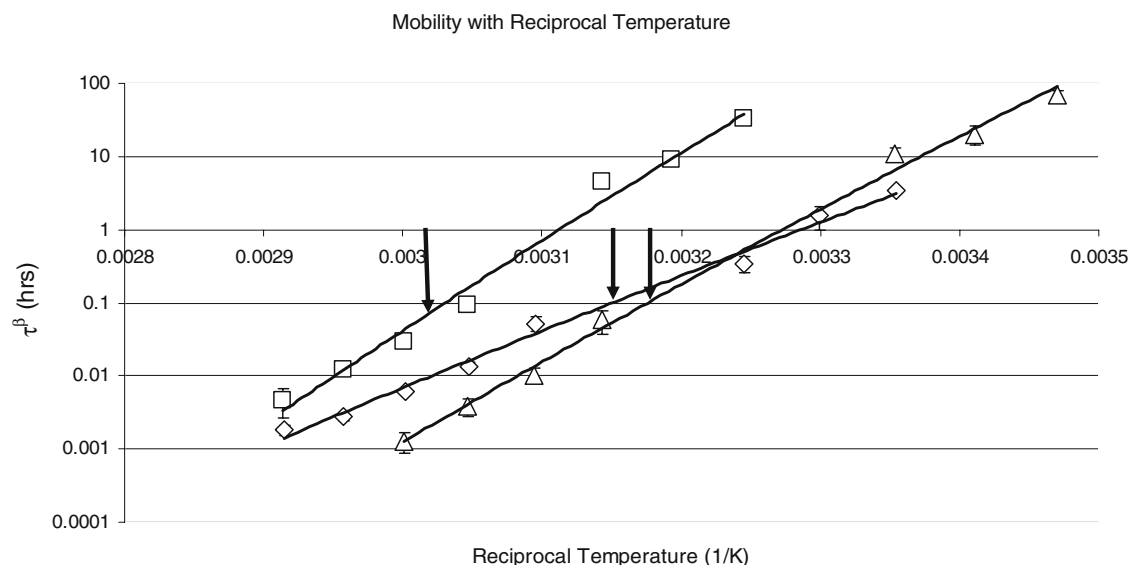
Fig. 9. Correlation of relaxation times for indomethacin (*diamonds*), flopropione (*squares*) and nifedipine (*triangles*). Relaxation times below T_g were measured using TAM for indomethacin and MDSC for nifedipine and flopropione. The *lines* are linear fits to the data. *Error bars* represent errors from three separate measurements. Indomethacin, $R^2 = 0.992$; flopropione, $R^2 = 0.987$; nifedipine, $R^2 = 0.996$. Error bars are sometimes smaller than the symbol. *Arrows* represent the T_g of respective compounds.

Table IV. Comparison Between Calorimetric Relaxation Times Obtained from Isothermal Microcalorimetry and Modulated DSC (in Hours) along with Enthalpic Relaxation and Recovery Obtained at Four Temperatures for Ketoconazole

Temperature (°C)	Isothermal Microcalorimetry MSE		Modulated DSC KWW	
	Enthalpy Relaxed (J/g)	Relaxation Time (τ^β)	Enthalpy Recovered (J/g)	Relaxation Time (τ^β)
20 (48 h)	5.4 ± 0.5	3.33 ± 1.1	2.1 ± 0.1	36 ± 5
25 (16 h)	3.1 ± 0.2	3.06 ± 0.6	2.0 ± 0.02	15 ± 1
30 (16 h)	3.3 ± 0.1	1.76 ± 0.2	2.8 ± 0.2	5.3 ± 0.5
35 (10 h)	1.7 ± 0.2	0.86 ± 0.2	1.8 ± 0.1	2.7 ± 0.2

The time in parenthesis is the longest time point for the experiment in modulated DSC and also the time point for comparison between the enthalpic relaxation and recovery. Data are average of three replicates except for the 20°C measurement where the number of replicates (TAM) was $n = 2$.

sucrose (35). Here, we extend the measurements to two more compounds, both of which are hydrophobic. Modulated DSC was used to evaluate the relaxation times for ketoconazole (temperatures 20, 25, 30 and 35°C) and Indomethacin (temperatures 25 and 30°C). The relaxation times were obtained using the protocol described previously for the other two compounds. It was found that, at all temperatures, the relaxation times obtained using scanning calorimetry (MDSC) were significantly higher than the relaxation times obtained using isothermal microcalorimetry. Tables IV and V give the comparison between the relaxation time constants (τ^β) obtained using the two techniques for ketoconazole and indomethacin, respectively. The tables also give comparisons between the enthalpic recovery obtained by integrating the non-reversing heat flow endothermic peak from MDSC for the last annealing time point, and enthalpic relaxation obtained by integrating the power time curve from TAM. If both calorimetric techniques are "seeing" the same relaxation processes, the enthalpy recovery should equal the integrated power time curve describing relaxation.

For obtaining enthalpic relaxation from TAM, data was initially analyzed using the time derivative of the MSE equation (35), given by Eq. 8. The MSE equation was used to generate the fitting curve which was extrapolated to time, $t = 0$. As described earlier, adjustment was made to account for the time spent by the sample in the thermal equilibration position. The MSE equation was chosen over the KWW equation because the MSE equation can be used for times approaching and including time zero, whereas the power in the derivative of the KWW equation approaches infinity as time approaches zero (35), which is unphysical and unacceptable. Enthalpy relaxation at longer times, where accurate power data are available, was obtained by integrating the area under the power–time curve. The enthalpic relaxation obtained using integrated TAM data, however, did not agree with the enthalpic recovery obtained from MDSC. For

ketoconazole at temperatures 20, 25 and 30°C the enthalpic relaxation obtained from the TAM data is significantly higher than the enthalpic recovery obtained from MDSC with the difference being greater at the lower temperature, while TAM data are comparable to DSC data at 35°C. Similar trends were seen for both the temperatures studied for Indomethacin as shown in Table V. The data suggest that the TAM is measuring some type of relaxation, perhaps beta-like relaxation or the fast relaxation components of the alpha distribution, which the enthalpy recovery experiment does not measure. However, there is also the possibility of systematic experimental error. We note that while we attempt to properly estimate the relaxation that occurs before we record accurate TAM data, we do so by extrapolation, and the enthalpy relaxation we estimate by extrapolation of the MSE equation is not a small fraction of the total relaxation. Thus, if the MSE equation, which is parameterized by a fit to data at longer times, fails to represent relaxation at very short times, systematic error would result. While we believe the differences shown between DSC enthalpy recovery and TAM enthalpy relaxation generally exceeds the possible experimental error, including systematic errors, interpretations of such data cannot be conclusive.

An interesting observation was made when all the relaxation times for ketoconazole and indomethacin were plotted against reciprocal temperature. Both measures of calorimetric relaxation data, while divergent at low temperature, seem to meet at the glass transition and extrapolate directly into the dielectric relaxation data obtained above T_g. Moreover, the change in slope at T_g observed with the TAM data for ketoconazole disappears when data from MDSC is compared with dielectric data (Fig. 10a). Similar results (with respect to divergent data below T_g and both meeting with dielectric data from above T_g) were found for Indomethacin (Fig. 10b). The data for ketoconazole suggests that the fast dynamics predicted by the modified Adam–Gibbs theory in

Table V. Comparison Between Calorimetric Relaxation Times Obtained from Isothermal Microcalorimetry and Modulated DSC (in Hours) along with Enthalpic Relaxation and Recovery Obtained at Two Temperatures for Indomethacin

Temperature (°C)	Isothermal Microcalorimetry MSE		Modulated DSC KWW	
	Enthalpy Relaxed (J/g)	Relaxation Time (τ^β)	Enthalpy Recovered (J/g)	Relaxation Time (τ^β)
25 (16 h)	3.1 ± 0.1	3.4 ± 0.3	2.6 ± 0.1	12.0 ± 0.9
30 (16 h)	3.5 ± 0.2	1.5 ± 0.5	2.9 ± 0.11	4.4 ± 0.4

The time in parenthesis is the longest time point for the experiment in modulated DSC and also the time point for comparison between the enthalpic relaxation and recovery. Data are means of three replicates.
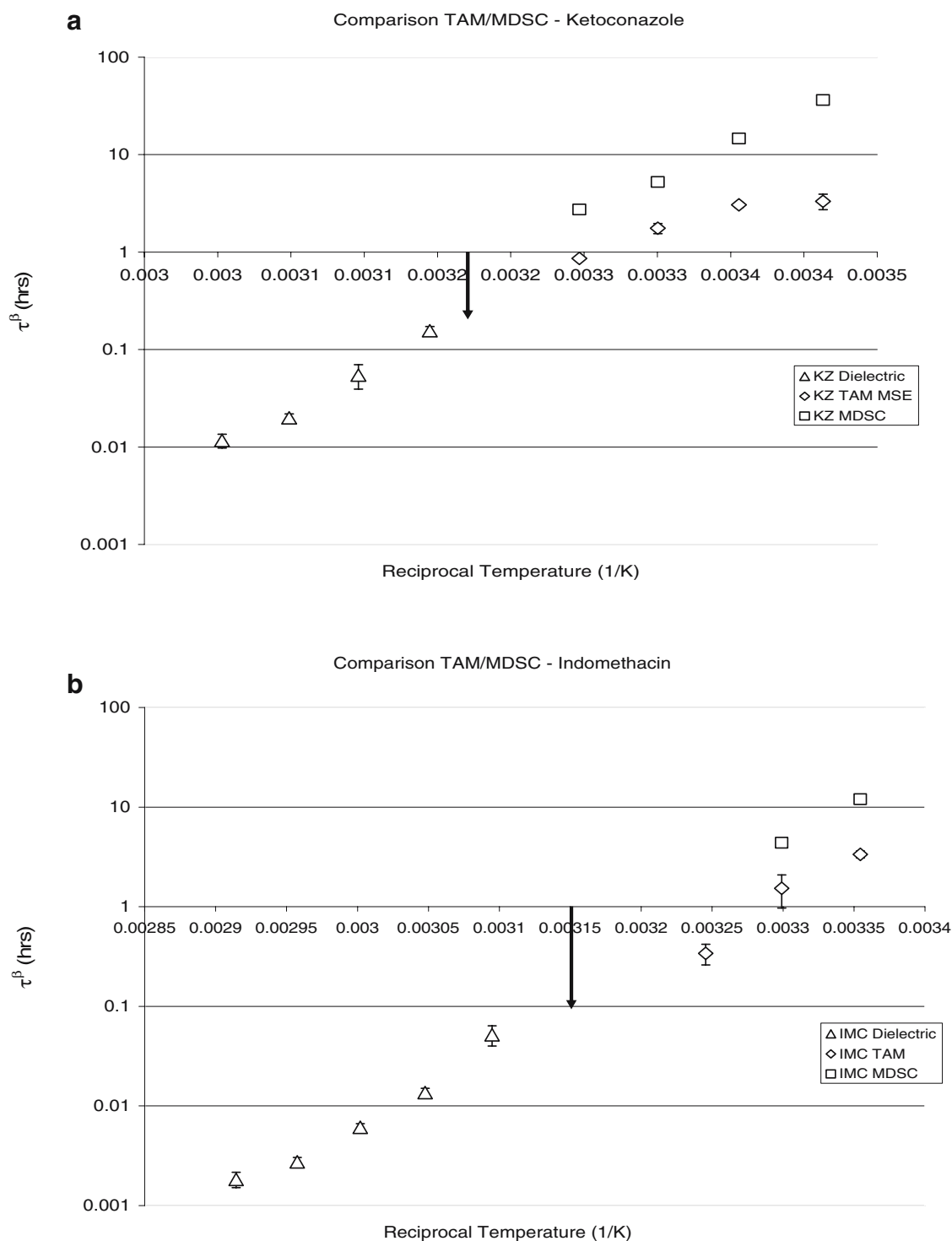
Fig. 10. (a) Correlation of dielectric relaxation times with different calorimetric relaxation times for ketoconazole. *Squares* represent calorimetric data from MDSC and *diamonds* represent calorimetric data from TAM. Dielectric data is common in both measurements and is represented by *triangles*. Error bars are sometimes smaller than the symbol. T_g is represented by the *arrow*. (b) Correlation of dielectric relaxation times with different calorimetric relaxation times for indomethacin. *Squares* represent calorimetric data from MDSC and *diamonds* represent calorimetric data from TAM. Dielectric data is common in both measurements and is represented by *triangles*. Error bars are sometimes smaller than the symbol. T_g is represented by the arrow.

the temperature range below the glass transition temperature (where the fictive temperature is higher than the actual temperature of the system causing faster relaxation) is also a function of the technique used to capture the relaxation in the glassy state. The more sensitive TAM is evidently capturing some of the faster motions which are not measured by the less sensitive DSC.

CONCLUSIONS AND PHARMACEUTICAL RELEVANCE

In this work the relaxation times for four glass formers with different properties was evaluated over a broad temperature range from T_g +25°C to T_g −25°C (approximately) using totally different techniques. The results show that the relaxation times obtained using one technique (dielectric relaxation spectroscopy) at temperatures above the glass transition temperature can be extrapolated to the relaxation times obtained using another technique/s (calorimetric, both scanning and isothermal) at temperatures below the glass transition temperature. That is, calorimetric and dielectric relaxation processes are roughly equivalent, or at least highly coupled. This result was not pre-ordained. Dielectric relaxation and calorimetric relaxation do reflect somewhat different types of mobility, rotational and mostly translational, respectively, and we might well have observed a large systematic difference between the dielectric and calorimetric relaxation times at a common temperature (i.e., T_g). However, the correspondence between relaxation times can be exploited for assessing pharmaceutical stability of amorphous formulations. For cases where the instability is dependent on molecular mobility, such correlations of relaxation times could be used as a predictive tool for estimating instability below the glass transition temperature at temperatures of pharmaceutical relevance. That is, relaxation times can be measured above (dielectric) and below (calorimetric) T_g, correlations between instability (i.e., crystallization) and dielectric relaxation can be established quickly at temperatures above T_g and given a calorimetric relaxation time determined at the temperature of pharmaceutical interest, an estimate of the stability can be made at this temperature. Of course, this procedure assumes that the coupling coefficient describing the correlation between instability and relaxation time does not depend on the measure of relaxation time (i.e., dielectric and calorimetric relaxations are equivalent).

However, before using such an approach, some caution is warranted. One has to make sure that when using the correlations between relaxation times for studying processes such as chemical degradation, the degradation mechanism is the same in both the temperature ranges (i.e., above the glass transition and below the glass transition temperature). For predicting physical instability, i.e., growth of crystals, one has to make sure that the same polymorph is being studied in both the temperature ranges. Finally, as stated earlier, the coupling between relaxation and instability that is observed above T_g (i.e., with dielectric methods) must also be valid for the type of relaxation being measured at temperatures well below T_g (i.e., by calorimetry). We have evaluated two techniques for measuring relaxation times below the glass transition temperature. Earlier research suggested that both these techniques, i.e., scanning (MDSC) and isothermal (TAM) calorimetry,

gave essentially the same relaxation times. However, present work suggests otherwise, with relaxation times from isothermal microcalorimetry being significantly smaller than those measured by scanning technique. The reasons for these observations are not clear at present, but the data suggest that the TAM is measuring, in part, some faster relaxation process in addition to the relaxation that is mobilized at the glass transition. However, which calorimetric relaxation time is most strongly coupled with "instability", and therefore would be most useful in stability prediction, is unknown at present, and is the subject of current research.

REFERENCES

1. P. Gupta, G. Chawla, and A. K. Bansal. Physical stability and solubility advantage from amorphous celecoxib: the role of thermodynamic quantities and molecular mobility. *Molecular Pharmaceutics* **1**(6):406–413 (2004).
2. J. Li, Y. Guo, and G. Zografi. The solid-state stability of amorphous quinapril in the presence of b-cyclodextrins. *J. Pharm. Sci.* **91**(1):229–243 (2002).
3. D. Zhou *et al.* Physical stability of amorphous pharmaceuticals: importance of configurational thermodynamic quantities and molecular mobility. *J. Pharm. Sci.* **91**(8):1863–1872 (2002).
4. Y. Aso, S. Yoshioka, and S. Kojima. Molecular mobility-based estimation of the crystallization rates of amorphous nifedipine and phenobarbital in poly(vinylpyrrolidone) solid dispersions. *J. Pharm. Sci.* **93**(2):384–391 (2004).
5. L. Carpentier, L. Bourgeois, and M. Descamps. Contribution of temperature modulated DSC to the study of the molecular mobility in glass forming pharmaceutical systems. *J. Therm. Anal. Calorim.* **68**(2):727–739 (2002).
6. S. Rambhatla, D. L.-B. A. Bakri, S. P. Duddu, K. Farinas, M. J. Pikal. Prediction of the onset of crystallization in amorphous pharmaceutical systems below the glass transition temperature. *AAPS Pharm. Sci.* 2000 AAPS Annual Meeting Supplement **2**(4) (Oct 2000).
7. M. D. Ediger, C. A. Angell, and S. R. Nagel. Supercooled liquids and glasses. *J. Phys. Chem.* **100**(31):13200–13212 (1996).
8. S. L. Shamblin *et al.* Characterization of the time scales of molecular motion in pharmaceutically important glasses. *J. Phys. Chem. B* **103**(20):4113–4121 (1999).
9. L. -M. Wang, V. Velikov, and C. A. Angell. Direct determination of kinetic fragility indices of glassforming liquids by differential scanning calorimetry: kinetic *versus* thermodynamic fragilities. *J. Chem. Phys.* **117**(22):10184–10192 (2002).
10. X. C. Tang, M. J. Pikal, and L. S. Taylor. A spectroscopic investigation of hydrogen bond patterns in crystalline and amorphous phases in dihydropyridine calcium channel blockers. *Pharm. Res.* **19**(4):477–483 (2002).
11. C. Bhugra, M. J. Pikal, and R. Shmeis. Crystallization and Relaxation Behavior of Melt Quenched Indomethacin Role of Mechanical Stress. Abstract, NERDG 2005, Rocky Hill, CT, 2005.

12. C. S. Lo, C. F. Wang, and H. C. Hsu. A stability-indicating HPLC assay method of indomethacin and the stability of indomethacin gels. *Zhonghua Yaoxue Zazhi* **45**(4):321–328 (1993).
13. C. Liu and G. Chen. Determination and stability of nifedipine injection by HPLC. *Yaowu Fenxi Zazhi* **13**:314–317 (1993).
14. E. Mikami *et al*. Rapid determination of drugs in pharmaceutical preparations by liquid chromatography. (VIII). Determination of ambroxol hydrochloride, prazosin hydrochloride, homochlorcyclizine hydrochloride, piroxicam, flopropione and pentoxifylline in pharmaceutical preparations. *Iyakuhin Kenkyu* **27**(9):626–631 (1996).
15. L. V. Allen Jr. and M. A. Erickson 3rd. Stability of ketoconazole, metolazone, metronidazole, procainamide hydrochloride, and spironolactone in extemporaneously compounded oral liquids. *American Journal of Health-System Pharmacy: AJHP: Official Journal of the American Society of Health-System Pharmacists* **53**(17):2073–2078 (1996).
16. G. P. Simon. Dielectric relaxation spectroscopy of thermoplastic polymers and blends. *Materials Forum* **18**:235–264 (1994).
17. J. Mijovic and J.-W. Sy. Molecular dynamics during crystallization of poly(L-lactic acid) as studied by broad-band dielectric relaxation spectroscopy. *Macromolecules* **35**(16):6370–6376 (2002).
18. R. He and D. Q. Craig. An investigation into the thermal behaviour of an amorphous drug using low frequency dielectric spectroscopy and modulated temperature differential scanning calorimetry. *J. Pharm. Pharmacol.* **53**(1):41–48 (2001).
19. J. Alie *et al*. Dielectric study of the molecular mobility and the isothermal crystallization kinetics of an amorphous pharmaceutical drug substance. *J. Pharm. Sci.* **93**(1):218–233 (2004).
20. S. P. Duddu and T. D. Sokoloski. Dielectric analysis in the characterization of amorphous pharmaceutical solids. 1. Molecular mobility in poly(vinylpyrrolidone)–water systems in the glassy state. *J. Pharm. Sci.* **84**(6):773–776 (1995).
21. J. Mijovic. Monitoring crystallization by dielectric spectroscopy. In *Dielectrics Newsletter*, 1998. pp. 1–3.
22. F. I. Mopsik. Precision time domain dielectric spectrometer. *Rev. Sci. Instrum.* **55**(1):79–87 (1984).
23. P. Debye. *Polar Molecules*, The Chemical Catalog Company Inc, New York, 1929.
24. K. S. Cole and R. H. Cole. Dispersion and absorption in dielectrics I. Alternating current characteristics. *J. Chem. Phys.* **9**(4):341–351 (1941).
25. D. W. Davidson and R. H. Cole. Dielectric relaxation in glycerol, propylene glycol, and *n*-propanol. *J. Chem. Phys.* **19**:1484–1490 (1951).
26. S. Havriliak and S. Negami. A complex plane representation of dielectric and mechanical relaxation processes in some polymers. *Polymer* **8**(4):appendix 206–210 (1967).
27. R. P. Auty and R. H. Cole. Dielectric properties of ice and solid D[sub 2]O. *J. Chem. Phys.* **20**(8):1309–1314 (1952).
28. D. W. Davidson and R. H. Cole. Dielectric relaxation in glycerol. *J. Chem. Phys.* **18**:1417 (1950).
29. G. Williams and D. C. Watts. Non-symmetrical dielectric relaxation behavior arising from a simple empirical decay function. *Trans. Faraday Soc.* **66**(1):80–85 (1970).
30. C. A. Angell *et al*. Relaxation in glassforming liquids and amorphous solids. *J. Appl. Physi.* **88**(6):3113–3157 (2000).
31. S. L. Shamblin *et al*. Interpretation of relaxation time constants for amorphous pharmaceutical systems. *J. Pharm. Sci.* **89**(3):417–427 (2000).
32. Z. Jiang, C. T. Imrie, and J. M. Hutchinson. Temperature modulated differential scanning calorimetry part IV. Effect of heat transfer on the measurement of heat capacity using quasi-isothermal ADSC. *J. Therm. Anal. Calorim.* **64**(1):85–107 (2001).
33. S. Weyer, A. Hensel, and C. Schick. Phase angle correction for TMDSC in the glass-transition region. *Thermochim. Acta* **304–305**:267–275 (1997).
34. K. Kawakami and M. J. Pikal. Calorimetric investigation of the structural relaxation of amorphous materials: evaluating validity of the methodologies. *J. Pharm. Sci.* **94**(5):948–965 (2005).
35. J. Liu *et al*. Dynamics of pharmaceutical amorphous solids: the study of enthalpy relaxation by isothermal microcalorimetry. *J. Pharm. Sci.* **91**(8):1853–1862 (2002).
36. K. Kawakami. Investigation of the structural relaxation process of amorphous formulation by isothermal microcalorimetry. *Netsu Sokutei* **31**(2):74–79 (2004).
37. W. Kauzmann. The nature of the glassy state and the behavior of liquids at low temperatures. *Chem. Rev. (Washington, DC, United States)* **43**:219–256 (1948).
38. N. l. T. Correia *et al*. Molecular mobility and fragility in indomethacin: a thermally stimulated depolarization current study. *Pharm. Res.* **18**(12):1767–1774 (2001).
39. S. Vyazovkin and I. Dranca. Physical stability and relaxation of amorphous indomethacin. *J. Phys. Chem. B* **109**(39):18637–18644 (2005).
40. I. M. Hodge. Adam–Gibbs formulation of enthalpy relaxation near the glass transition. *J. Res. Natl. Inst. Stand. Technol.* **102**(2):195–205 (1997).
41. V. Andronis and G. Zografi. The molecular mobility of super-cooled amorphous indomethacin as a function of temperature and relative humidity. *Pharm. Res.* **15**(6):835–842 (1998).
42. B. C. Hancock, S. L. Shamblin, and G. Zografi. Molecular mobility of amorphous pharmaceutical solids below their glass transition temperatures. *Pharm. Res.* **12**(6):799–806 (1995).
43. E. Fukuoka, M. Makita, and S. Yamamura. Some physicochemical properties of glassy indomethacin. *Chem. Pharm. Bull.* **34**(10):4314–4321 (1986).